Journal of Electroceramics, 9, 117–124, 2002

Evolution of Structure and Dielectric Properties on Bismuth-Based Pyrochlore with TiO_2 Incorporation

HUILING DU & XI YAO

Electronic Materials Research Laboratory, Xi'an Jiaotong University, Xi'an 710049, People's Republic of China

Submitted December 3, 2001; Revised September 18, 2002; Accepted October 1, 2002

Abstract. The lattice constant and thermal expansion of the pyrochlore oxides $(Bi_{1.5}Zn_{0.5})(Zn_{0.5-x/3}Ti_x Sb_{1.5-2x/3})O_7$ $(0 \leq x \leq 1.5)$ were studied by X-ray powder diffraction, SEM and IR spectra, respectively. The average grain size is enhanced as the Ti-doping level is increased. The XRD results indicate that all samples have a cubic structure (*Fd*3*m* space group) with the lattice parameter decreasing with rising Ti content. The variation of lattice parameters with composition was found to obey Vegard's law. The assignments for the absorption bands in the IR spectra of the series of samples have also been given. The results of diffraction patterns and IR spectra demonstrated that these compounds have the cubic pyrochlore structure. The dielectric properties of the samples were systematically studied. Dielectric constant and temperature coefficient of dielectric constant exhibit strong dependence on the Ti concentration. Dielectric constant varies sharply from 30 when $x = 0$ to 115 when $x = 1.5$.

Keywords: pyrochlore oxides, lattice constant, IR spectra, dielectric properties

1. Introduction

Dielectric ceramics are widely used in microelectronic technologies and microwave communication. High dielectric constant ceramics have received intensive attention in reducing the size of microelectronic circuits, where low dielectric loss and near-zero temperature coefficient of the dielectric constant are required for many applications. In recent years, many researchers have focused on the application of high frequency dielectrics, such as those in the Ba-Nd-Ti-O system and Bi-Zn-Nb-O system. Bismuth-based pyrochlores exhibit well-known useful properties for multilayer capacitors. Compounds of the general formula $A_2B_2O_7$ (where A is a trivalent or bivalent cation and B is tetravalent or pentavalent cation) represent a family of phases with the pyrochlore structure. Pyrochlore oxides display a remarkable range of physical properties, including (for specific compositions) metallic, semiconducting, or ionic electrical behavior that can be controlled by doping [1–4]. Other properties include dielectric character, ferroelectric behavior, ferrimagnetism, and giant magnetoresistance. The crystal structure of those oxides has been described by many authors [5–7]. A wide variety of additional cations are commonly found to be incorporated in pyrochlore solid solutions in specimens that occur in nature.

The pyrochlore structure is closely related to fluorite and can be considered as an ordered defective fluorite. It exhibits space group *Fd*3*m* with eight formula units within the cubic unit cell. The ions occupy four crystallographically nonequivalent positions: A at 16d, B at 16c, O at 48f and O′ at 8b. There is an interstitial site that, within this space group, is at 8a.

As a member of the pyrochlore family of compounds, bismuth zinc niobate is a typical high frequency dielectric with high permittivity and low dielectric loss, and can be applied in various devices, such as temperature-stable multilayer ceramics capacitors and microwave resonators and filters [8–10]. Much work has been performed on improving the dielectric properties, especially in enhancing the permittivity and reducing dielectric loss [11, 12]. Among them, Sn and Ti substitution in the bismuth zinc niobate (BZN) system was studied and reported recently [13, 14].

In the present work, the influence of Ti concentration on the lattice constant, thermal expansion and dielectric properties of $Bi_{1.5}ZnSb_{1.5}O_7$ ceramics was investigated. The aim of this work was to study the structure and dielectric properties of materials with tetravalent titanium substituted into bismuth pyrochlore.

2. Experimental Procedure

2.1. Sample Preparation and Characterization

The samples were prepared by the conventional solid state reaction method. High-purity powders of Bi_2O_3, ZnO, Sb_2O_3 and TiO_2 were used as raw materials. These four ingredients were weighed according to the compositions: $(Bi_{1.5}Zn_{0.5})(Zn_{0.5-x/3}Ti_xSb_{1.5-2x/3})O_7$ ($x = 0, 0.25, 0.5, 1.0, 1.5$). They were mixed and ground for 4 h in a ball mill with deionized water, then dried and calcined at 800°C for 2 h. After being reground, the powders were pressed into discs of 12 mm in diameter and 1 mm in thickness with a small amount of polyvinyl ethanol binder. Subsequently, these discs were sintered at temperature between 1050 to 1200°C for 2 h in air and then furnace-cooled.

The densities of the sintered discs were determined by the liquid displacement method. The average densities obtained were 94–96% of the theoretical values. Crystalline phases in the sintered samples were identified by X-ray powder diffraction technique (XRD), using a Rigaku D/MAX-2400 X-ray diffractometer with Cu K_α radiation. The microstructure of the samples was examined on well-sintered surfaces using an AMARY 1000 scanning electron microscope (SEM).

2.2. Dielectric Properties Measurements

Low-fire silver electrodes were used for dielectric measurements. The dielectric constant and dissipation factor of $(Bi_{1.5}Zn_{0.5})(Zn_{0.5-x/3}Ti_xSb_{1.5-2x/3})O_7$ were measured using a high precision LCR meter (HP 4284A). Resistivity data were obtained using a HP 4339A high-resistance meter at a measuring voltage of 100 V. The temperature dependence of the dielectric constant was measured at four different frequencies (10 K, 100 K and 1 MHz) and temperature varying from RT to 450°C by placing the discs in an automated measurement system consisting of a PC computer, a HP 4284A LCR meter and a temperature chamber.

3. Results and Discussion

3.1. Microstructure and Crystal Structure

Figure 1 shows the microstructures observed in specimens prepared in the $(Bi_{1.5}Zn_{0.5})(Zn_{0.5-x}Sb_{1.5-2x}Ti_{3x})O_7$ system. Apparently, Ti concentration has resulted in a significant change in the grain growth behavior in series samples sintered in air. Increasing the Ti incorporation in the compositions, the grain size is increased remarkably. The average grain size of BZST continuously increases from no more than 2 μm to about 8 μm with increasing Ti content from $x = 0$ to 1.5.

In these compounds, the ionic radius of Zn^{2+}, Sb^{5+} and Ti^{4+} with six-coordination are 0.75, 0.61 and 0.605 Å, respectively [15]. In view of the similar radii for Sb and Ti, it is possible to assume that Ti doping can be fully incorporated into the pyrochlore structure of $(Bi_{1.5}Zn_{0.5})(Zn_{0.5}Sb_{1.5})O_7$. The average ionic radii of the various amounts of Zn^{2+}, Sb^{5+} and Ti^{4+} at B-site in the lattice is shown in Table 1. Hence, the ratio of the ionic radii of the cation at the A-site to that at the B-site is about 1.50–1.53, this value is just in the region of the tolerance factor for the pyrochlore compounds proposed by Subramanian et al. [5]. The zinc ion is positive divalent, animony ion is positive pentavalent and titanium ion is positive tetravalent. It is assumed that Ti^{4+} can co-substitute Zn^{2+} and Sb^{5+} at the B-site. The mechanism of substitution can be presented: $3Ti^{4+} \rightarrow Zn^{2+} + 2Sb^{5+}$. Therefore, the criterion of the charge neutrality can also be satisfied.

The X-ray diffraction patterns for all of the compounds shown in Fig. 2 were recorded using Cu K_α radiation. All the reflections in the diffractogram can be indexed with respect to the cubic pyrochlore phase of space group *Fd*3*m*. There are several small peaks in the $x = 1.5$ pattern suggests the presence of a secondary phase. It is difficult to identify the phase due to its minor amounts.

Figure 2 also shows the shift of the (222) reflection of the cubic pyrochlore phase. An apparent shift of the (222) reflection to the right with an increase in the x value was observed. This indicates that the size of the cubic pyrochlore cell changes with the Ti content. The lattice constant of the pyrochlore phase was determined by the extrapolation method from a Nelson-Riley plot and is shown as a function of composition in Table 1.

There is an almost linear relation between lattice constant and composition x as shown in Fig. 3. The

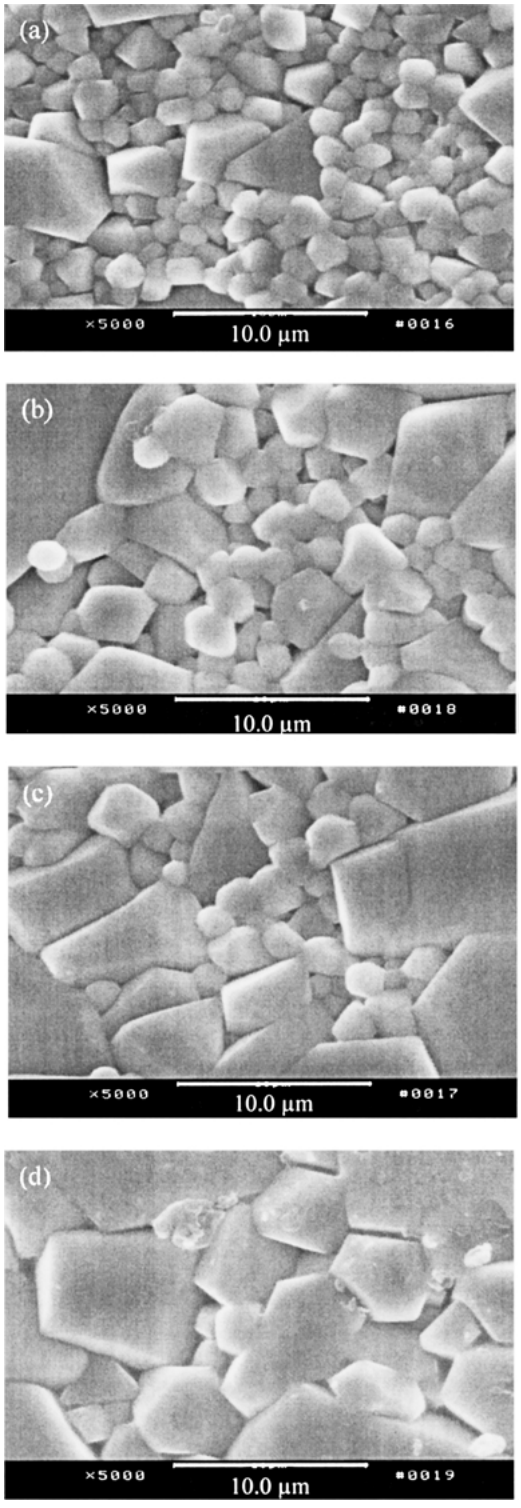

Fig. 1. Microstructure of BZST ceramics sintered at 1080°C in air for 2 h. (a) $x = 0.25$, (b) $x = 0.5$, (c) $x = 1.0$, and (d) $x = 1.5$.

lattice constant, a_0, is found to decrease linearly with the atomic fraction of the smaller tetravalent titanium cation in excellent agreement with Vegard's law. The decrease of the lattice constant is attributed to the slightly smaller size of the titanium ion compared with that of the antimony and zinc ion.

3.2. *IR Spectroscopy*

Infrared absorption spectroscopy can be used to characterize the compounds. The IR absorption bands of solids in the range 100–1000 cm^{-1} are usually assigned to vibrations of ions in the crystal lattice [16]. Above 1000 cm^{-1} no one-phonon absorption was observed and the ceramics became semi-transparent. The infrared lattice vibration frequencies of some pyrochlore compounds with a formula $A_2B_2O_7$ have been studied. There are seven IR-active optic modes in the infrared spectra of the pyrochlore oxides originating from vibration and bending of metal-oxygen bond [5]. The band (ν_1) at about 600 cm^{-1} is from the B—O stretching vibration in the BO_6 octahedron and the band (ν_2) at about 400 cm^{-1} is from the A—O stretching vibration. However, the assignments for the absorption bands in the infrared spectra of a pyrochlore compound with a formula $(A_{1.5}A'_{0.5})(B_{1.5}B'_{0.5})O_7$ have not been reported.

As Fig. 4 shows, there are two primary absorption bands in the range 400–1000 cm^{-1} of the infrared spectra of the studied samples. The band in the region 630–740 cm^{-1} can be ascribed to B—O stretching vibration and the band in the region 400–450 cm^{-1} can be attributed to A—O stretching vibration in the $AO_6O'_2$ polyhedron. Furthermore, two bands in the region 630–740 cm^{-1} can be distinguished clearly for the samples with low Ti concentration as marked in Fig. 4. This can be due to the presence of two different types of ions with distinct radius at the B-site of the pyrochlore unit cell. The two-mode behavior due to the presence of two different ions present at the B-site of complex pyrochlores unit cell has already been reported [17]. The assignment of the internal octahedral modes is based on the bonding character between B and O ions. The weightier the mass of the bonding atoms, the lower the stretching vibration frequency of the bond. The atomic weight of Sb^{5+} is larger than that of Zn^{2+}. Hence, the associated resonant frequency of Zn—O appears at the higher frequency compared to that of Sb—O vibration. In $(Bi_{1.5}ZnSb_{1.5})O_7$, the number of ZnO_6 octahedra is only one third of that of the SbO_6 octahedra. Thus,

Table 1. Structural parameter and thermal expansion coefficient of the compositions.

Composition (x)	Average radius of B-site (Å)	r_A/r_B	Lattice constant (a_0)	TEC (ppm/°C)	ν (A—O)	ν (B—O)
0	0.6450	1.5814	10.4444	9.478	414	664
0.25	0.6385	1.5974	10.4156	9.116	419	662
0.5	0.6321	1.6137	10.3899	9.088	426	652
1.0	0.6192	1.6474	10.3531	9.075	437	636
1.5	0.6063	1.6825	10.3062	9.833	446	634

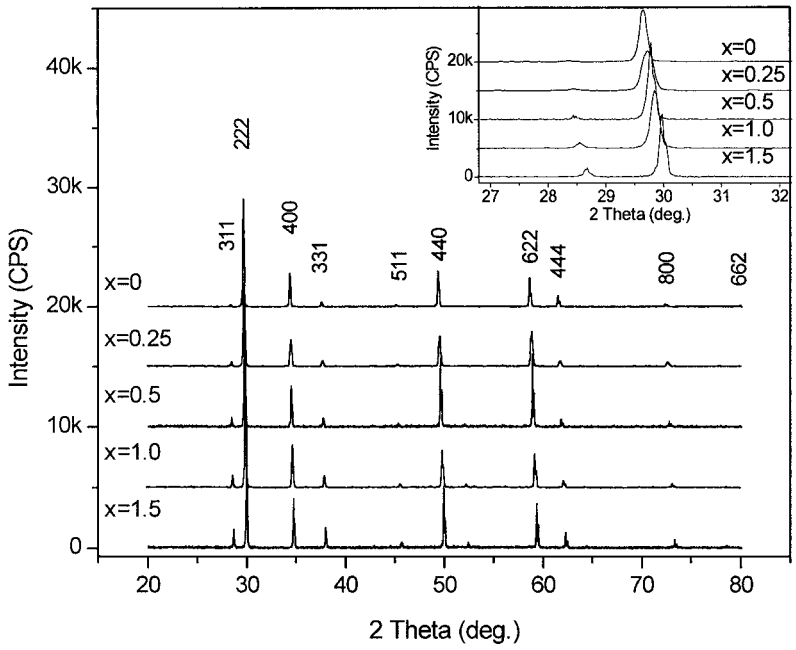

Fig. 2. XRD pattern of BZST ceramics. The inserted patterns with smaller x range.

the intensity of the absorption bands from the Zn—O stretching vibration will be weaker than that from the Sb—O stretching vibration.

With an increase in Ti concentration, it is observed that the absorption bands of Sb—O bond shift to lower frequency with gradual disappearance of the IR bands of the Zn—O bond. The frequency of the band maximum, ν(B—O), decreased almost linearly with the lattice constant a, or average radius of B-site (r_B), indicating that the B—O bond strengths weakens with a decrease in a_0 or r_B. However, the dependence of the B—O vibration frequency on the B ion has thus far been explained by an increase in force constant when the atomic number increases. In the present study we noticed a second trend to the above by our observation of the dependence of the B—O vibration on the size of the B ion. The smaller the B ion radius (with the same A ion) the lower the observed B—O vibrational frequency, indicating that the force constant has decreased. We know that pyrochlore oxides with different species in A or B site will form different configurations, in which the exact positions of atoms differ slightly [18]. Small distortions of the atomic positions affect the force constant of the vibrational modes resulting in small shifts in vibrational frequency.

Also from the IR spectra it can be noticed that the frequency of the absorption band of site A increases with increasing Ti concentration. The cell volume decrease associated with the replacement of larger ion (Sb^{5+} and Zn^{2+}) by smaller ion (Ti^{4+}) at the B-site has an appreciable influence on the bonding character of A—O bonds. It can be concluded that the IR spectra

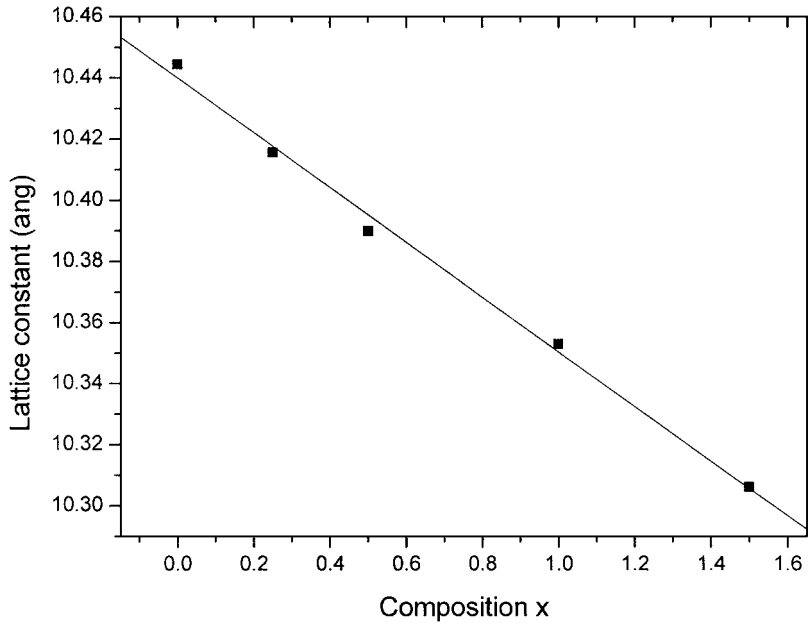

Fig. 3. The variation of lattice constant with x in BZST pyrochlores.

can give an idea about the change in the crystal structure of the pyrochlore due to the perturbation exerted on A—O bonds by introducing the Ti^{4+} ion. It is reasonable to assume that the electronic distribution of A—O bonds is affected when a Ti cation with $3d^2 4s^2$ orbital is introduced into its neighborhood and this consequently affects the vibrational frequency of the A—O bond.

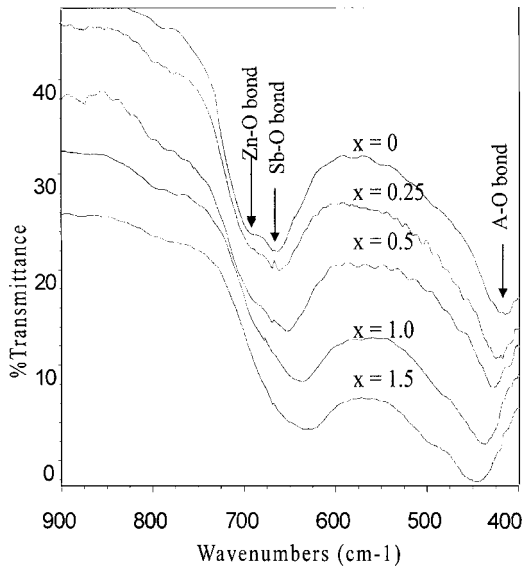

Fig. 4. FT-IR spectra of BZST ceramics with various x value.

3.3. *Dielectric Properties*

The dielectric properties of these ceramics are sensitive to the composition and sintering temperature. All of the ceramics exhibit low dielectric loss values. The temperature dependence of dielectric constant and dissipation factor at 1 MHz of BZST ceramics in a range of high temperatures are shown in Figs. 5 and 6, respectively. The dielectric constants of all the measured BZST series ceramics decreases to some extent with increasing temperature. The dielectric constant for BZS ceramics (where $x = 0$) is 30, and increases linearly with increasing Ti substitution up to 115 for high Ti content compositions (where $x = 1.5$). On the other hand, the temperature coefficient (α_c) effectively decreases from one end member ($\alpha_c = -93$ ppm/°C for $x = 0$) to the other end member ($\alpha_c = -611$ ppm/°C for $x = 1.5$). The tendencies of the dielectric behavior versus temperature for all samples are similar, with the large negative temperature coefficients for samples with higher Ti contents. The dielectric constant increased with the increase of the Ti^{4+} ions substitution, and show the maximum value of 115 at the $x = 1.5$ composition.

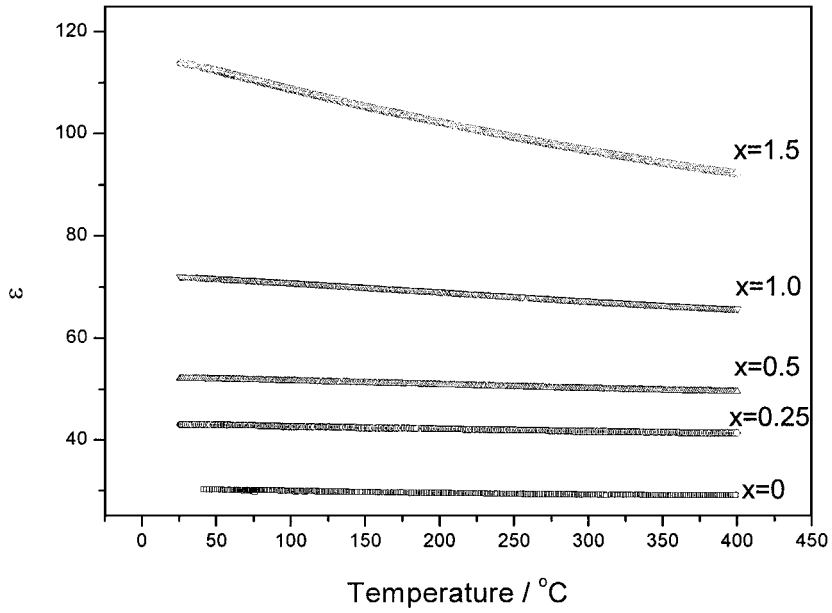

Fig. 5. The temperature dependence of dielectric constant at 1 MHz of BZST ceramics at high temperature range.

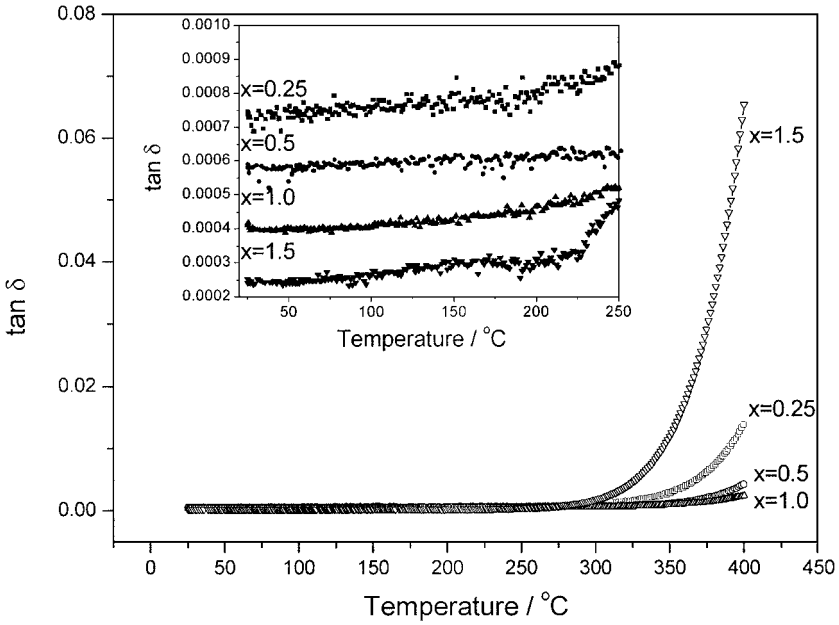

Fig. 6. The temperature dependence of dielectric loss at 1 MHz of BZST ceramics at high temperature range. The inserted patterns with smaller *y* range.

Ti incorporation in BZS pyrochlore also increased the temperature coefficient of dielectric constant.

As Ti-rich ceramics have the more interesting characteristics as we anticipated, the temperature dependence of dielectric properties at various frequencies were studied. Figure 7 shows the variation of the dielectric constant and dissipation factor of BZST4 ceramics with temperature, at several selected

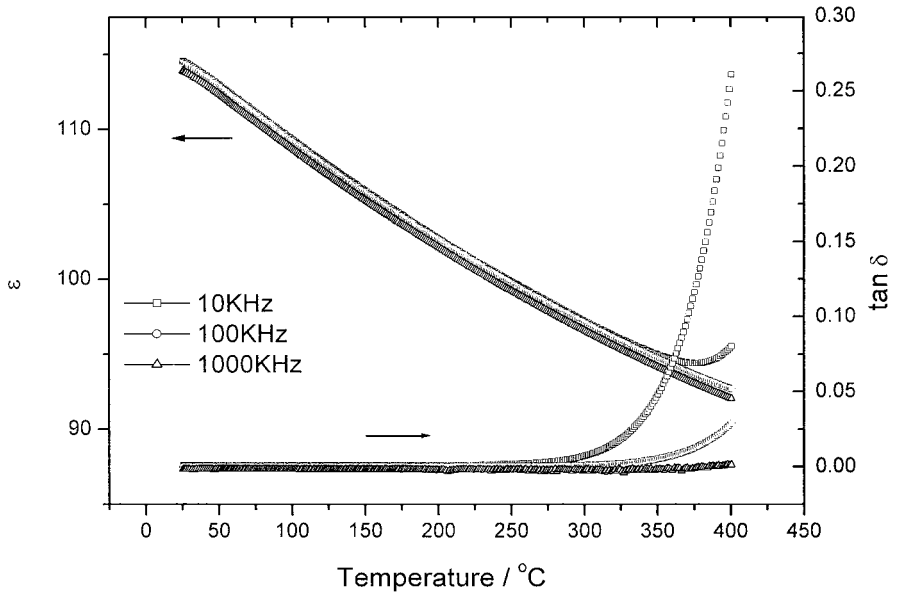

Fig. 7. The variation of the dielectric constant and dissipation factor of BZST4 ceramics with temperature, at various frequencies.

frequencies. It can be noticed that tan δ remains at small values over a broader temperature range at high frequencies than at lower frequencies. The dielectric constants at various frequencies almost overlap and decrease linearly with temperature. The general trends of ε' and tan δ appreciably increase at temperatures above 300°C, which typically associate with losses by conduction [19]. On increasing the temperature, the electrical conductivity increases due to the increase in thermally activated drift mobility of electric charge carriers according to the hopping conduction mechanism. Therefore, the dielectric polarization increases causing a marked increase in ε and tan δ as the temperature increases.

We know that dielectrics with high ε are based on structures with BO_6-octahedra joined one to another by their tops. The key ion B located in the center of octahedra plays an important role in determining dielectric properties. The strong correlation between highly-polarizable octahedra not only provides high ε, but also causes a critical temperature dependence of dielectric constant. As to our pyrochlore dielectrics, it is believed that there is a strong correlation when some kind of ion such as Ti^{4+} or Nb^{5+} is placed into the center of octahedra and would result in high ε and large α_ε. Relatively weak correlation occurs between octahedra where Sb^{5+} is located, brings on low ε and small α_ε.

4. Conclusions

A new series of the pyrochlore compounds $(Bi_{1.5}Zn_{0.5})(Zn_{0.5-x}Sb_{1.5-2x}Ti_{3x})O_7$ $(0 \leq x \leq 1.5)$ has been synthesized by solid state reaction processing. The incorporation of Ti^{4+} into the bismuth zinc antimonate ceramics induced the decrease of lattice constant while remaining cubic pyrochlore phase due to the smaller ionic radius of Ti^{4+} compared to Sb^{5+} and Zn^{2+}. The vibrational frequency of B—O bond evaluated from the stretching IR band decreased almost linearly with increasing Ti concentration, indicating that the B—O bond strength weakens with a decrease in a_0 or r_B.

Dielectric properties vary remarkably with composition in Ti-incorporated ceramics. With Ti substitution, the dielectric constant increases significantly while the temperature coefficient shifted to larger negative value.

References

1. H.L. Tuller and P.K. Moon, *Mat. Sci. Eng.* B, **1**, 171 (1988).
2. Brendan J. Kennedy, *Mater. Res. Bull.*, **32**, 479 (1997).
3. Y. Shimakawa, Y. Kubo, and T. Manako, *Nature*, **379**, 53 (1996).
4. B.J. Kennedy and T. Vogt, *J. Solid State Chem.*, **126**, 261 (1996).
5. M.A. Subramanian, G. Aravamudan, and G.V. Subba Rao, *Solid State Chem.*, **15**, 55 (1983).

6. Ismunandar, J. Brendan Kennedy, and A. Brett Hunter, *Mater. Res. Bull.*, **34**, 1263 (1999).
7. C. Bryan Chakoumakos, *Solid State Chem.*, **53**, 120 (1984).
8. M.F. Yan, H.C. Ling, and W.W. Rhodes, *J. Am. Ceram. Soc.*, **73**, 1106 (1990).
9. Du Huiling, Wang Hong, and Yao Xi, *Ferroelectrics Letters*, **28**, 35 (2001).
10. Ren Wei, S. Trolier McKinstry, C.A. Randall, and T.R. Shrout, *J. Appl. Phys.*, **89**, 767 (2001).
11. Du Huiling, Wang Hong, Xu Lijun and Yao Xi, *J. Chin. Ceram. Soc.*, **28**, 210 (2000) (in Chinese).
12. D.P. Cann, C.A. Randall, and T.R. Shrout, *Solid State Commu.*, **100**, 529 (1996).
13. Du Huiling, Yao Xi, and Zhang Liangying, *Ceram. Inter.*, **28**, 231 (2002).
14. M. Valant and P.K. Davies, *J. Am. Ceram. Soc.*, **34**, 5437 (1999).
15. R.D. Shannon, *J. Acta. Cryst.* A, **32**, 751 (1976).
16. V.A.M. Brabers, *Phys. Status Solidi*, **33**, 563 (1969).
17. F.W. Poulsen, M. Glerup, and P. Holtappels, *Solid State Ionics* **135**, 595 (2000).
18. B.J. Kennedy, *Physics* B, **241–243**, 303 (1998).
19. S.A. Mazen, M.H. Abdallah, B.A. Sabrah, and H.A. Hashem, *Phys. Status Solidi*, **134**, 263 (1992).